

# Detecting keV-Range Super-Light Dark Matter Using Graphene Josephson Junction

Doojin Kim,<sup>1,2,\*</sup> Jong-Chul Park,<sup>3,†</sup> Kin Chung Fong,<sup>4,5</sup> and Gil-Ho Lee<sup>6</sup>

<sup>1</sup>*Mitchell Institute for Fundamental Physics and Astronomy,*

*Department of Physics and Astronomy, Texas A&M University, College Station, TX 77843, USA*

<sup>2</sup>*Department of Physics, University of Arizona, Tucson, AZ 85721, USA*

<sup>3</sup>*Department of Physics, Chungnam National University, Daejeon 34134, Republic of Korea*

<sup>4</sup>*Raytheon BBN Technologies, Quantum Information Processing Group, Cambridge, MA 02138, USA*

<sup>5</sup>*Department of Physics, Harvard University, Cambridge, MA 02138, USA*

<sup>6</sup>*Department of Physics, Pohang University of Science and Technology, Pohang 37673, Republic of Korea*

We propose a new dark matter detection strategy that will enable the search of super-light dark matter  $m_\chi \simeq 0.1$  keV, representing an improvement of the minimum detectable mass by more than three order of magnitude over the ongoing experiments. This is possible by integrating intimately the target material,  $\pi$ -bond electrons in graphene, into a Josephson junction to achieve a high sensitivity detector that can resolve a small energy exchange from dark matter as low as  $\sim 0.1$  meV. We investigate detection prospects with mg-scale and g-scale detectors by calculating the scattering rate between dark matter and the free electrons confined in two-dimensional graphene with Pauli blocking factors included. We find not only that the proposed detector can serve as a complementary probe of super-light dark matter but also achieve higher experimental sensitivities than other proposed experiments, i.e. in having a low detectable threshold provided the same target mass, thanks to the extremely low energy threshold of our Josephson junction sensor.

## I. INTRODUCTION

While dark matter is a crucial ingredient of the universe and its cosmological history (see also Ref. [1] for a recent review), the elusive nature of dark matter renders its detection via non-gravitational interactions rather challenging. A host of theoretical and experimental effort has been devoted to understanding the weakly interacting massive particles (WIMPs), mainly motivated by the so-called WIMP miracle. The null signal observations thus far sets stringent bounds on dark matter candidates of  $m_\chi \sim 10$  GeV – 100 TeV [2]. On the other hand, the dark matter mass can range, in general, from  $10^{-22}$  eV to  $10^{68}$  eV [2], so the spotlight is directing gradually toward other mass scales.

Dark matter candidates lying in the keV-to-MeV mass range have received particular attention. Most of the conventional dark matter direct detection experiments are nearly insensitive to the associated signal due to the energy threshold to overcome, and thus relevant dark matter models are less constrained. Moreover, thermal production of such dark matter is still allowed. Many models containing dark matter candidates of this mass scale have been proposed and addressing various interesting phenomenology; for example, self-/strongly-interacting dark matter [3, 4], dark matter freeze-in production [5, 6], keV mirror-neutrino dark matter [7], MeV dark matter for the 511 keV  $\gamma$ -ray line [8], MeV secluded dark matter [9, 10], keV dark matter for the 3.5 keV X-ray line [11, 12], and

elastically decoupling dark matter [13].

Direct searches of MeV-range light dark matter are being actively performed by e.g., DAMIC [14], DarkSide [15], SENSEI [16], SuperCDMS [17], and XENON [18] Collaborations. However, experimental detection of keV-range “super-light” dark matter is very challenging as the expected energy deposition is of order meV – eV, requiring a tiny energy threshold. A handful of detection schemes have been proposed thus far [19–30], based on new technologies measuring small energy depositions in the detector. They assume that dark matter scatters off either electrons [19, 20, 22, 25, 26, 29, 30], nuclei [21, 23, 24] or phonons [27, 28] in the detector material. Various detector materials were investigated, including superconducting devices [19, 20, 30], superfluid helium [21, 23, 24], graphene [22, 29], carbon nanotube [25], three-dimensional Dirac materials [26] and polar materials [27, 28]. Although some of them may accommodate dark matter events invoking meV-range energy depositions, the actual detection is essentially limited by the bolometer technology. The aforementioned proposals adopt sensors such as a transition edge sensor (TES) [31], a microwave kinetic inductance device (MKID) [32], and a superconducting-nanowire single-photon detector (SNSPD) [33, 34], with typical operation frequencies ranging from X-ray to near-infrared [35], from X-ray to far-infrared [36], and from ultraviolet to mid-infrared [37], respectively. To detect the energy deposition from dark matter as small as meV, i.e.  $\sim 240$  GHz, further R&D is therefore needed.

To extend the search of dark matter in lower mass regime, which has never been explored by dark matter direct searches, we propose a new experimental strategy

\* doojin.kim@tamu.edu

† jcpark@cnu.ac.kr

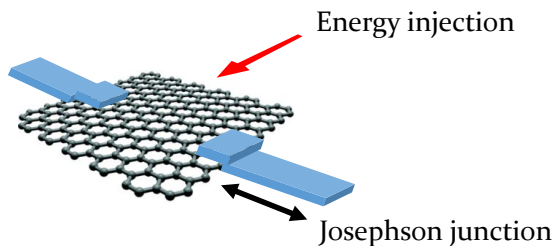


FIG. 1. A schematic description of detection principle. When injected energy raises the electron temperature in the graphene sheet, the calorimetric effect can switch the zero-voltage of Josephson junction to resistive state with an appropriate level of bias current.

using a graphene-based Josephson junction microwave single-photon detector [38]. It was recently demonstrated in the laboratory that the GJJ device can have an energy resolution equivalent to sub-meV energy quanta [39]. Therefore, it is possible to design and embark on experiments aiming at detecting dark matter of  $m_\chi \gtrsim 0.1$  keV, using a sensor of higher Technology Readiness Level. We provide a conceptual detector design proposal and study the detection prospects of super-light dark matter interacting with  $\pi$ -bond electrons not only at the proposed detector but at its smaller-version prototype.

## II. DETECTION PRINCIPLE

A single unit of the device consists of a sheet of mono-layer graphene two sides of which are joined to superconducting material, forming a superconductor-normal metal-superconductor (SNS) Josephson junction (JJ) [38], as schematically shown in Figure 1. Basically, when injected energy raises the electron temperature in the graphene sheet, the calorimetric effect can switch the zero-voltage of JJ to resistive state with an appropriate level of bias current. Graphene is a mono-atomic layer of carbon atoms in a hexagonal structure [40, 41]. Its electronic band structure shows linear energy-momentum dispersion relationship which resembles to that of massless Dirac fermions in two-dimension. Near the Dirac point where the density of state vanishes, electronic heat capacity also vanishes. Due to the extremely suppressed electronic heat capacity of mono-layer graphene and its constricted thermal conductance to its phonons, the device is highly sensitive to small energy deposition. Very recently, Lee *et al.* [39] have demonstrated a microwave bolometer using GJJ with a noise equivalent power (NEP) corresponding to the thermodynamic limit. This NEP infers to the energy resolution of single 32-GHz (or equivalently,  $\sim 0.13$  meV) microwave photon in a single-photon detection mode.

If dark matter of interest couples to electrons, it can scatter off  $\pi$ -bond free electrons in the graphene sheet, transferring some fraction of its incoming kinetic energy. The recoiling electron heats up and thermalizes

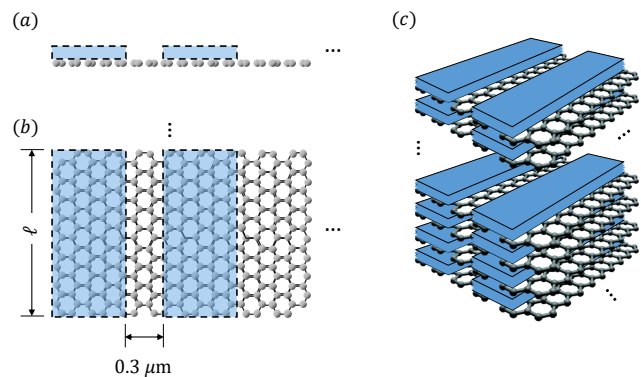


FIG. 2. A conceptual design for the proposed GJJ dark matter detector. (a) Lateral view of a single detector unit. (b) Top view of a single detector unit.  $\ell = 3 \mu\text{m}$  ( $\ell = 30 \mu\text{m}$ ) corresponds to a threshold energy of 0.1 meV (1 meV). (c) Full detector made of a stack of detector units.

with nearby electrons rapidly via electron-electron interactions within a few picoseconds [42, 43], and the JJ is triggered. The dark matter in the present universe floats around the earth with the typical velocity being  $\sim 10^{-3}c$ . Therefore, a dark matter particle of order 1 keV carries a kinetic energy of order 1 meV [ $\approx 1 \text{ keV} \times (10^{-3})^2$ ] so that the GJJ device can possess the sensitivity to the signal induced even by sub-keV-range dark matter. To the best of our knowledge, no device ever known has exhibited the sensitivity of this level practically, so we expect that the microwave single-photon detector technology using GJJ enables us to explore parameter regions for super-light particle dark matter in the near future.

## III. CONCEPTUAL DESIGN PROPOSAL

Inspired by the GJJ device, we propose a dark matter detector which consists of a multitude of the GJJ devices. A single detector unit is the assembly of a graphene sheet and a number of superconducting material strips with a length of  $\ell$ . The strips of  $\ell = 3 \mu\text{m}$  ( $\ell = 30 \mu\text{m}$ ) corresponding to a threshold energy of 0.1 meV (1 meV) are laid on a graphene sheet by an interval of  $0.3 \mu\text{m}$ , showing an array of superconducting-graphene-superconducting-graphene-superconducting- $\dots$  (SGSGS $\dots$ ). When the strip length increases, the area of graphene increases so the heat capacity also increases. Therefore, more energy is needed to trigger the GJJ device. Each sequence of SGS represents a single GJJ device. Figure 2(a) and Figure 2(b) display schematic layouts of the detector unit from one side and top, respectively. A full detector can be made of a stack of such detector units as schematically depicted in Figure 2(c).

Our sensitivity study is based on a g-scale detector, while a mg-scale prototype detector can be prepared first to test the feasibility of larger-scale detectors. To prepare for the units forming a mg-scale graphene device, one needs a total of  $\sim 1 \text{ m} \times 1 \text{ m}$  sheet of graphene, which

can be grown by chemical vapor depositions [44, 45].

Since the GJJ bolometer is extremely sensitive to small changes in temperature, it is crucial to keep the system temperature low enough to suppress potential thermal backgrounds or noise. To this end, we place the detector in the cryogenic surroundings by cooling the detector system down to  $\sim 10$  mK using dilution refrigerators. An irreducible background may arise from the solar neutrinos (mostly  $pp$  neutrinos) scattering off an electron and depositing a small amount of energy [46]. However, considering the volume of the detector at hand, the expected number of background events is negligible ( $\lesssim \mathcal{O}(10^{-3})$  g $^{-1}$ year $^{-1}$ ) [20, 47].

We remark that in our study here the proposed detector plays a role of not only the bolometer to measure the temperature change or the single-photon detector to count the number of scattering events, but target material off which dark matter scatters. Alternatively, this can be used only for a bolometer or a single-photon detector in other dark matter detection proposals by coupling it to the target material such as superconductors, superfluid helium, or polar materials in Refs. [20], [21], and [27], respectively. In this case, energetic quasiparticles generated in the target material by dark matter get absorbed into graphene, followed by increasing the electronic temperature of the graphene and triggering GJJ.

#### IV. EXPERIMENTAL SENSITIVITIES

We are now in the position to study dark matter signal sensitivities which would be achieved by the proposed GJJ detector. Our interest here is the interaction between dark matter and  $\pi$ -bond electrons in the graphene which can behave like free electrons. Indeed, dark matter may deposit energy via scattering off the  $\sigma$ -bond electrons, making an additional contribution to the signal sensitivity. However, we conservatively restrict our analysis to the former channel to demonstrate the usefulness of the GJJ-based detector as a super-light dark matter detector, while deferring a full analysis for a future publication.

While our sensitivity calculations closely follow the procedure formulated in Refs. [19, 20], we modify them wherever the two-dimensional nature of graphene is relevant. The total expected event count per unit mass per unit time,  $n_{\text{eve}}$  is given by

$$n_{\text{eve}} = \int dE_r dv_{\chi\parallel} \frac{d\langle n_{\text{gr}}^e \sigma v_{\text{rel}\parallel} \rangle}{dE_r} \frac{1}{a_{\text{gr}}} \frac{\rho_{\chi}}{m_{\chi}} f_{\text{MB}}(v_{\chi\parallel}), \quad (1)$$

where  $n_{\text{gr}}^e$  is the number density of target electrons per unit area and  $a_{\text{gr}} = 7.62 \times 10^{-8}$  g $\cdot$ cm $^{-2}$  is the areal density of graphene.  $m_{\chi}$  is the mass of dark matter and  $\rho_{\chi}$  is the local dark matter energy density which is chosen to be 0.3 GeV $\cdot$ cm $^{-3}$  throughout our analysis.  $f_{\text{MB}}(v_{\chi\parallel})$  is the graphene-surface-parallel velocity profile of dark matter for which we take a plane-projection

of a modified Maxwell-Boltzmann distribution [48] with root-mean-square velocity  $v_0 = 220$  km $\cdot$ s $^{-1}$  and escape velocity  $v_{\text{esc}} = 500$  km $\cdot$ s $^{-1}$  (see Appendix):

$$f_{\text{MB}}(v_{\chi\parallel}) = \frac{2(e^{-v_{\chi\parallel}^2/v_0^2} - e^{-v_{\text{esc}}^2/v_0^2})}{\sqrt{\pi}v_0 \operatorname{erf}(v_{\text{esc}}/v_0) - 2v_{\text{esc}}e^{-v_{\text{esc}}^2/v_0^2}}. \quad (2)$$

Finally, the velocity-averaged event rate on a (sufficiently thin) graphene sheet per unit time  $\langle n_{\text{gr}}^e \sigma v_{\text{rel}\parallel} \rangle$  is

$$\langle n_{\text{gr}}^e \sigma v_{\text{rel}\parallel} \rangle = \int \frac{d^3 p_{\chi,f}}{(2\pi)^3} \frac{|\overline{\mathcal{M}}|^2}{16m_e^2 m_{\chi}^2} S_{\text{gr}}(E_r, q), \quad (3)$$

where  $p_{\chi,f}$  is the momentum of final-state dark matter and where all the total energy quantities are taken in the non-relativistic limit. Here  $|\overline{\mathcal{M}}|^2$  denotes the matrix element for the scattering process between dark matter and free electrons. The Pauli blocking effects are encoded in  $S_{\text{gr}}(E_r, q)$ , a structure function over electron recoil kinetic energy  $E_r$  and the magnitude of momentum transfer along the graphene surface  $q = |\vec{p}_{\chi\parallel,i} - \vec{p}_{\chi\parallel,f}|$  with subscript  $i$  implying the initial state. It is then convenient to convert  $d^3 p_{\chi,f}$  to  $dE_r$  and  $dq$ :

$$\frac{d^3 p_{\chi,f}}{(2\pi)^3} \longrightarrow \frac{dE_r dq}{(2\pi)^2} \frac{2q(E_{\chi,i} - E_r)}{\tilde{\lambda}(q^2, p_{\chi,i}^2, p_{\chi,f}^2)}, \quad (4)$$

where  $\tilde{\lambda}(x, y, z) = \sqrt{2(xy + yz + zx) - x^2 - y^2 - z^2}$  and where we integrate out  $p_{\chi,f}^z$  by pulling out the delta function factor in  $S_{\text{gr}} = (2\pi)\delta(p_{\chi,i}^z - p_{\chi,f}^z) \cdot S$  (see Appendix). We next take the analytic expression for  $S$  derived in Ref. [20] based on Ref. [49]:

$$S(E_r, q) = \frac{m_e^2 T}{\pi q} \left[ \frac{E_r/T}{1 - \exp(-E_r/T)} \left( 1 + \frac{\xi}{E_r/T} \right) \right], \quad (5)$$

where  $T$  is the system temperature surrounding the detector which we take to be 10 mK as mentioned earlier. The  $\xi$  quantity is given by

$$\xi = \log \left[ \frac{1 + e^{(\epsilon_- - \mu)/T}}{1 + e^{(\epsilon_- + E_r - \mu)/T}} \right] \quad (6)$$

with

$$\epsilon_- = \frac{1}{4} \frac{\{E_r - q^2/(2m_e)\}^2}{q^2/(2m_e)}. \quad (7)$$

Here  $\mu$  is the chemical potential which is identified as the Fermi energy  $E_F$  at zero temperature. For a two-dimensional object like graphene, the linear energy-momentum dispersion suggests

$$E_F = v_F \sqrt{\pi n_c}. \quad (8)$$

Here the Fermi velocity of graphene  $v_F$  is 1.15  $\times 10^8$  cm $\cdot$ s $^{-1}$  [50] and carrier density  $n_c$  is chosen to be 10 $^{12}$  cm $^{-2}$  [39].

We assume that dark matter interacts with electrons via an exchange of mediator  $\phi$  whose mass is  $m_\phi$ , as in many of the preceding studies. In the non-relativistic limit, the scattering cross section between free electrons and say, fermionic dark matter  $\chi$  is given by

$$\sigma_{e\chi} \approx \frac{g_e^2 g_\chi^2}{\pi} \frac{\mu_{e\chi}^2}{(m_\phi^2 + q^2)^2}, \quad (9)$$

where  $g_e$  and  $g_\chi$  parameterize couplings of  $\phi$  to electrons and  $\chi$  and where  $\mu_{e\chi}$  is the reduced mass of the electron- $\chi$  system. If the mediator is heavy enough such that  $m_\phi^2 \gg q^2$ , Eq. (9) is simplified to

$$\sigma_{e\chi}^{\text{heavy}} \approx \frac{g_e^2 g_\chi^2}{\pi} \frac{\mu_{e\chi}^2}{m_\phi^4}. \quad (10)$$

On the other hand, for the opposite limit or the light mediator case (i.e.,  $m_\phi^2 \ll q^2$ ), we get

$$\sigma_{e\chi}^{\text{light}} \approx \frac{g_e^2 g_\chi^2}{\pi} \frac{\mu_{e\chi}^2}{q^4}. \quad (11)$$

The matrix element in Eq. (3) is related to the scattering cross section in Eq. (9) as

$$\sigma_{e\chi} = \frac{1}{16\pi} \frac{|\overline{\mathcal{M}}|^2}{m_e^2 m_\chi^2} \mu_{e\chi}^2. \quad (12)$$

To estimate our sensitivity reach, we take Eqs. (10) and (11) as the reference cross sections. For the light mediator case, we replace the  $q$ -dependence by a reference value  $q_{\text{ref}} = \alpha_e m_e$  with  $\alpha_e$  being the usual electromagnetic fine structure constant, following the prescription in Refs. [30, 47].

Figure 3 displays the sensitivities of the proposed GJJ detector to 0.1 keV – 0.1 GeV dark matter in the plane of dark matter mass  $m_\chi$  and scattering cross section  $\sigma_{e\chi}$ . For estimating the sensitivity reach, we require 3.6 signal events which correspond to the 95% C.L. upper limit under the assumption of a null event observation over negligible neutrino-induced background events with Poisson statistics [52]. As mentioned before, such dark matter is assumed to interact with the  $\pi$ -bond electrons in the graphene target through an exchange of  $\phi$ . The top and the bottom panels are for the heavy and the light mediator cases, respectively. In both panels, the blue (red) curves show the sensitivities with electron kinetic energy deposition being in-between 0.1 meV and 0.1 eV (1 meV and 1 eV), i.e., the superconducting strips of the GJJ detector have  $\ell = 3 \mu\text{m}$  ( $\ell = 30 \mu\text{m}$ ). The dashed curves are the expected results with a 1 g-scale detector exposed for a year, whereas the solid curves the ones corresponding to a 1 mg-scale prototypical detector. For the heavy mediator case, we exhibit the existing bounds (gray region) together from DAMIC [14], DarkSide-50 [15], SENSEI [16], SuperCDMS [17], XENON10 [51], and XENON1T [18] by the orange, purple, cyan, pink, brown, and green

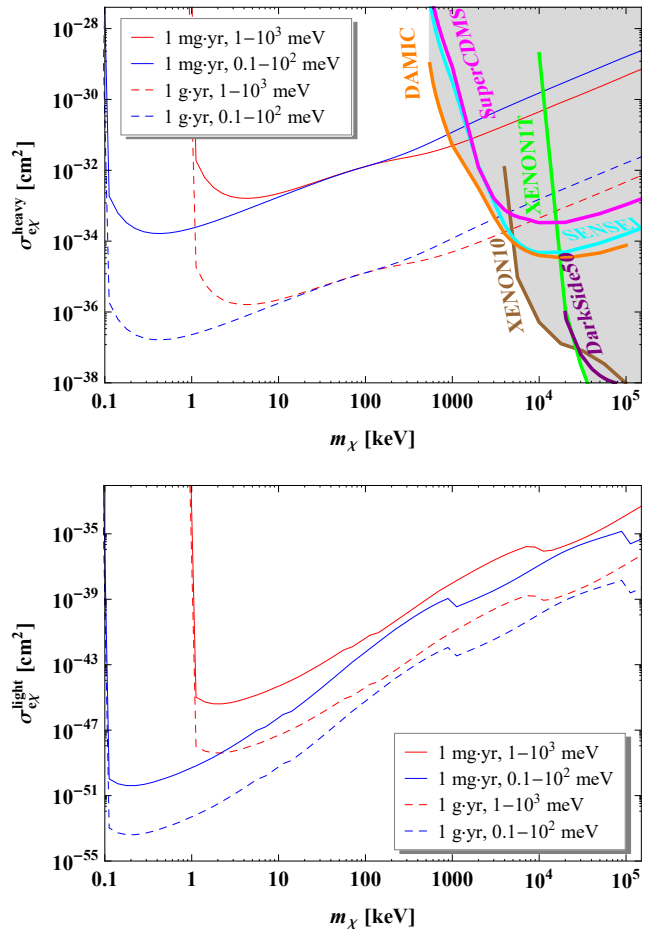


FIG. 3. Sensitivities of the proposed GJJ detector to 0.1 keV – 0.1 GeV dark matter in the plane of dark matter mass  $m_\chi$  and scattering cross section between dark matter and electrons  $\sigma_{e\chi}$ . The dark matter is assumed to scatter off  $\pi$ -bond electrons in graphene, which can behave like free electrons, via an exchange of a heavy mediator (top panel) or a light mediator (bottom panel). Blue (red) curves show the sensitivities with electron kinetic energy deposition falling in 0.1 meV – 0.1 eV (1 meV – 1 eV), and dashed (solid) curves are for a 1 g (1 mg) GJJ detector with one-year exposure. For comparison, existing limits for the heavy mediator case are shown together: DAMIC [14], DarkSide-50 [15], SENSEI [16], SuperCDMS [17], XENON10 [51], and XENON1T [18]. Existing limits for the light mediator case appear outside the displayed region.

lines, respectively. The current limits for the light mediator case are set by DAMIC [14], DarkSide-50 [15], SENSEI [16], SuperCDMS [17], and XENON10 [51], but they appear outside the displayed region.

## V. DISCUSSIONS

While the aforementioned dark matter direct search experiments are exploring  $m_\chi - \sigma_{e\chi}$  space, cosmological

and astrophysical observations provide bounds on super-light dark matter. For example, the so-called Lyman- $\alpha$  forest is a powerful tool to constrain keV-range dark matter which was thermally produced in the early universe. Such “warm” dark matter behaves relativistically when freezes out, so it may affect the structure formation, leaving appreciable differences in the Lyman- $\alpha$  absorption features from what is observed today (see, for example, Ref. [53]). Currently, warm dark matter of  $m_\chi \lesssim \mathcal{O}(\text{keV})$  is disfavored by Lyman- $\alpha$  forests, while there still exist relatively large uncertainties even among very recent results: e.g., Ref. [54] claims that  $m_\chi > 10$  keV is allowed at 95% C.L., whereas Ref. [55] claims  $m_\chi > 1.9$  keV is allowed at 95% C.L.. In fact, the proposed GJJ detector enables to probe 1 – 10 keV dark matter very efficiently by lowering the threshold to 0.1 meV, as compared to dark matter detectors adopting other bolometer technologies. This is because a lower threshold allows to access the phase space associated with recoil electrons carrying smaller energy. This is also clearly demonstrated by the red (higher threshold) and the blue (lower threshold) curves in Figure 3.

By contrast, if dark matter is produced non-thermally, the bounds from the Lyman- $\alpha$  forest are generically not relevant. It is therefore important to explore the  $\mathcal{O}(\text{keV})$  mass region in a model-independent sense. There are many well-motivated physics models containing such non-thermal super-light dark matter candidates: for example, sterile neutrinos [56, 57], super-light dark gauge bosons [58–60], axion-like dark matter particles [61–63], axino/gravitino dark matter [62, 64]. We expect that search strategies using the proposed GJJ detector can provide a probe complementary to the existing experimental effort for such dark matter candidates.

Finally, we point out that the proposed detector is capable of detecting even lighter dark matter candidates of sub-meV – eV mass. For example, axion-like particle or dark gauge boson dark matter candidates within such a mass range can be absorbed to the detector material via a Compton-like process with an electron resulting in an emission of a photon, i.e.,  $\chi + e \rightarrow \gamma + e$ . Here the radiated photon is typically as energetic as the mass energy of the incoming dark matter, so the proposed detector may have decent sensitivities to these dark matter candidates. Note that if the mass of the absorbed dark matter particle is greater than the binding energy of an electron, i.e.,  $\mathcal{O}(\text{eV})$ , an electron is ejected via a process analogous to the photoelectric effect [65–68]. Numerous dark matter direct detection experiments have conducted searches for such ejected electron signals [14, 16–18, 69–80], and our proposal can offer a new avenue for this search effort.

## VI. CONCLUSIONS

In conclusion, we have proposed a class of *new* dark matter detectors, adopting the GJJ device which has been implemented and demonstrated experimentally.

Due to its outstanding sensitivity to energy changes as small as  $\sim 0.1$  meV, the proposed detectors made of an array of GJJ devices are, for the first time, capable of probing dark matter candidates as light as  $\sim 0.1$  keV via the scattering of dark matter off electrons. We have shown that the sensitivity of detectors of 1-g graphene can reach  $\sigma_{e\chi} \approx 10^{-37}$  cm $^{-2}$  and  $\sigma_{e\chi} \approx 10^{-54}$  cm $^{-2}$  for the heavy and the light mediator cases, with one-year exposure. We are now planning to develop a prototypical detector of bigger SNS JJ multiplicity, along with more dedicated background studies and extended investigations of various dark matter candidates which can be detected by the proposed detectors.

## ACKNOWLEDGMENTS

We would like to thank Kaustubh Agashe, Bhaskar Dutta and Yue Zhao for their careful reading of the draft and insightful discussions. We also would like to thank Rupak Mahapatra and Yonit Hochberg for their useful comments and discussions. This work was performed in part at the Aspen Center for Physics, which is supported by National Science Foundation grant PHY-1607611. Part of this work was discussed in the workshop “Dark Matter as a Portal to New Physics” at the Asia Pacific Center for Theoretical Physics in 2020. The work of DK was supported in part by the Department of Energy under Grant DE-FG02-13ER41976 (de-sc0009913) and is supported in part by the Department of Energy under Grant de-sc0010813. The work of JCP is supported by the National Research Foundation of Korea (NRF-2019R1C1C1005073 and NRF-2018R1A4A1025334). KCF acknowledges the support from the Army Research Office under Cooperative Agreement Number W911NF-17-1-0574. GHL acknowledges the support from Samsung Science and Technology Foundation (Project No. SSTF-BA1702-05).

## APPENDIX

**Projected Maxwell-Boltzmann distribution.** - When a dark matter particle of velocity  $v_\chi$  is incident on a graphene sheet by angle  $\theta$ , the parallel component, i.e.,  $v_{\chi\parallel} = v_\chi \cos \theta$ , is involved in the momentum transfer. Utilizing the fact that  $\cos \theta$  is a flat variable, we find that the dark matter number distribution in  $v_{\chi\parallel}$  for a given  $v_\chi$  is

$$\left. \frac{dN_\chi}{dv_{\chi\parallel}} \right|_{v_\chi} = \frac{dN_\chi}{d\cos\theta} \frac{d\cos\theta}{dv_{\chi\parallel}} = \frac{1}{2v_\chi}. \quad (13)$$

The whole distribution  $f_{\text{MB}}(v_{\chi\parallel})$  is obtained by convolving Eq. (13) with the probability density of  $v_\chi$  given by a modified Maxwell-Boltzmann distribution [48]:

$$f_{\text{MB}}(v_{\chi\parallel}) \propto \int_{v_{\chi\parallel}}^{v_{\text{esc}}} dv_\chi \frac{1}{v_\chi} v_\chi^2 e^{-v_\chi^2/v_0^2}, \quad (14)$$

which results in the expression in Eq. (2).

**Structure function.** - The structure function for the graphene system of interest  $S_{\text{gr}}$  is given by

$$S_{\text{gr}}(E_r, q) = 2 \int \frac{d^3 p_{e,i}}{(2\pi)^3} \int \frac{d^3 p_{e,f}}{(2\pi)^3} (2\pi) \delta(p_{e,i}^z - p_{e,f}^z) \\ \times (2\pi)^4 \delta^{(4)}(p_{\chi,i} + p_{e,i} - p_{\chi,f} - p_{e,f}) \\ \times f_{e,i}(E_{e,i}) \{1 - f_{e,f}(E_{e,f})\}, \quad (15)$$

where  $p_{e,i(f)}$  denotes the momentum of the initial-state (final-state) electron. The delta function in the first line reflects the assumption that the free electrons are confined in the graphene surface, or equivalently, they do not get any significant momentum change along the surface-normal direction, as far as the electron recoil kinetic energy is sufficiently smaller than the work function of graphene. The Fermi-Dirac distribution functions for

the initial-state (final-state) electrons  $f_{e,i(f)}$  are

$$f_{e,i(f)} = \left\{ 1 + \exp\left(\frac{E_{e,i(f)} - \mu}{T}\right) \right\}^{-1}, \quad (16)$$

where  $\mu$  and  $T$  are the chemical potential and the system temperature, respectively. Integrating over  $d^3 p_{e,f}$  in combination with the spatial components of the four-dimensional delta function yields

$$S_{\text{gr}}(E_r, q) = (2\pi) \delta(p_{\chi,i}^z - p_{\chi,f}^z) \cdot \frac{1}{2\pi^2} \int d^3 p_{e,i} \\ \times \delta(E_r + E_{\chi,i} - E_{\chi,f}) f_{e,i}(E_{e,i}) \{1 - f_{e,f}(E_{e,f})\} \\ \equiv (2\pi) \delta(p_{\chi,i}^z - p_{\chi,f}^z) \cdot S(E_r, q), \quad (17)$$

where we factor out the delta function of  $p_{\chi,f}^z$ , which is used for the  $d^3 p_{\chi,f}$  integral, and separately define  $S(E_r, q)$ . The closed form for  $S(E_r, q)$  is available in the non-relativistic limit [49], as shown in Eq. (5).

- 
- [1] G. Bertone and D. Hooper, *Rev. Mod. Phys.* **90**, 045002 (2018).
- [2] M. Battaglieri et al. (2017) arXiv:1707.04591 [hep-ph].
- [3] E. D. Carlson, M. E. Machacek, and L. J. Hall, *Astrophys. J.* **398**, 43 (1992).
- [4] Y. Hochberg, E. Kuflik, T. Volansky, and J. G. Wacker, *Phys. Rev. Lett.* **113**, 171301 (2014), arXiv:1402.5143 [hep-ph].
- [5] T. Moroi, H. Murayama, and M. Yamaguchi, *Phys. Lett.* **B303**, 289 (1993).
- [6] L. J. Hall, K. Jedamzik, J. March-Russell, and S. M. West, *JHEP* **03**, 080 (2010), arXiv:0911.1120 [hep-ph].
- [7] Z. G. Berezhiani and R. N. Mohapatra, *Phys. Rev.* **D52**, 6607 (1995), [279(1995)], arXiv:hep-ph/9505385 [hep-ph].
- [8] C. Boehm, D. Hooper, J. Silk, M. Casse, and J. Paul, *Phys. Rev. Lett.* **92**, 101301 (2004), arXiv:astro-ph/0309686 [astro-ph].
- [9] J.-H. Huh, J. E. Kim, J.-C. Park, and S. C. Park, *Phys. Rev.* **D77**, 123503 (2008), arXiv:0711.3528 [astro-ph].
- [10] M. Pospelov, A. Ritz, and M. B. Voloshin, *Phys. Lett.* **B662**, 53 (2008), arXiv:0711.4866 [hep-ph].
- [11] J.-C. Park, S. C. Park, and K. Kong, *Phys. Lett.* **B733**, 217 (2014), arXiv:1403.1536 [hep-ph].
- [12] D. Kim and J.-C. Park, *Phys. Lett.* **B750**, 552 (2015), arXiv:1508.06640 [hep-ph].
- [13] E. Kuflik, M. Perelstein, N. R.-L. Lorier, and Y.-D. Tsai, *Phys. Rev. Lett.* **116**, 221302 (2016), arXiv:1512.04545 [hep-ph].
- [14] A. Aguilar-Arevalo et al. (DAMIC), *Phys. Rev. Lett.* **123**, 181802 (2019), arXiv:1907.12628 [astro-ph.CO].
- [15] P. Agnes et al. (DarkSide), *Phys. Rev. Lett.* **121**, 111303 (2018), arXiv:1802.06998 [astro-ph.CO].
- [16] O. Abramoff et al. (SENSEI), *Phys. Rev. Lett.* **122**, 161801 (2019), arXiv:1901.10478 [hep-ex].
- [17] R. Agnese et al. (SuperCDMS), *Phys. Rev. Lett.* **121**, 051301 (2018), [erratum: *Phys. Rev. Lett.* 122, no. 6, 069901 (2019)], arXiv:1804.10697 [hep-ex].
- [18] E. Aprile et al. (XENON1T), *Phys. Rev. Lett.* **123**, 251801 (2019), arXiv:1907.11485 [hep-ex].
- [19] Y. Hochberg, Y. Zhao, and K. M. Zurek, *Phys. Rev. Lett.* **116**, 011301 (2016), arXiv:1504.07237 [hep-ph].
- [20] Y. Hochberg, M. Pyle, Y. Zhao, and K. M. Zurek, *JHEP* **08**, 057 (2016), arXiv:1512.04533 [hep-ph].
- [21] K. Schutz and K. M. Zurek, *Phys. Rev. Lett.* **117**, 121302 (2016), arXiv:1604.08206 [hep-ph].
- [22] Y. Hochberg, Y. Kahn, M. Lisanti, C. G. Tully, and K. M. Zurek, *Phys. Lett.* **B772**, 239 (2017), arXiv:1606.08849 [hep-ph].
- [23] S. Knapen, T. Lin, and K. M. Zurek, *Phys. Rev.* **D95**, 056019 (2017), arXiv:1611.06228 [hep-ph].
- [24] H. J. Maris, G. M. Seidel, and D. Stein, *Phys. Rev. Lett.* **119**, 181303 (2017), arXiv:1706.00117 [astro-ph.IM].
- [25] G. Cavoto, F. Luchetta, and A. D. Polosa, *Phys. Lett.* **B776**, 338 (2018), arXiv:1706.02487 [hep-ph].
- [26] Y. Hochberg, Y. Kahn, M. Lisanti, K. M. Zurek, A. G. Grushin, R. Ilan, S. M. Griffin, Z.-F. Liu, S. F. Weber, and J. B. Neaton, *Phys. Rev.* **D97**, 015004 (2018), arXiv:1708.08929 [hep-ph].
- [27] S. Knapen, T. Lin, M. Pyle, and K. M. Zurek, *Phys. Lett.* **B785**, 386 (2018), arXiv:1712.06598 [hep-ph].
- [28] S. Griffin, S. Knapen, T. Lin, and K. M. Zurek, *Phys. Rev.* **D98**, 115034 (2018), arXiv:1807.10291 [hep-ph].
- [29] E. Baracchini et al. (PTOLEMY), (2018), arXiv:1808.01892 [physics.ins-det].
- [30] Y. Hochberg, I. Charaev, S.-W. Nam, V. Verma, M. Colangelo, and K. K. Berggren, (2019), arXiv:1903.05101 [hep-ph].
- [31] D. H. Andrews, W. F. Brucksch, W. T. Ziegler, and E. R. Blanchard, *Review of Scientific Instruments* **13**, 281 (1942).
- [32] P. K. Day, H. G. LeDuc, B. A. Mazin, A. Vayonakis, and J. Zmuidzinas, *Nature* **425**, 817 (2003).
- [33] A. D. Semenov, G. N. Goltsman, and A. A. Korneev, *Physica C: Superconductivity* **351**, 349 (2001).
- [34] G. N. Goltsman, O. Okunev, G. Chulkova, A. Lipatov, A. Semenov, K. Smirnov, B. Voronov, A. Dzardanov, C. Williams, and R. Sobolewski, *Applied Physics Letters*

- 79**, 705 (2001).
- [35] T. Gerrits, A. Lita, B. Calkins, and S. W. Nam, “Superconducting transition edge sensors for quantum optics,” in *Superconducting Devices in Quantum Optics*, edited by R. H. Hadfield and G. Johansson (Springer International Publishing, 2016) pp. 31–60.
- [36] J. Zmuidzinas, *Annual Review of Condensed Matter Physics* **3**, 169 (2012).
- [37] I. Holzman and Y. Ivry, *Technol.* **2019**, 1800058 (2018), arXiv:1807.09060 [physics.ins-det].
- [38] E. D. Walsh, D. K. Efetov, G.-H. Lee, M. Heuck, J. Crossno, T. A. Ohki, P. Kim, D. Englund, and K. C. Fong, *Phys. Rev. Applied* **8**, 024022 (2017).
- [39] G.-H. Lee, D. K. Efetov, L. Ranzani, E. D. Walsh, T. A. Ohki, T. Taniguchi, K. Watanabe, P. Kim, D. Englund, and K. C. Fong, (2019), arXiv:1909.05413 [cond-mat].
- [40] K. S. Novoselov, A. K. Geim, S. V. Morozov, D. Jiang, M. I. Katsnelson, I. V. Grigorieva, S. V. Dubonos, and A. A. Firsov, *Nature* **438**, 197 (2005), arXiv:cond-mat/0509330 [cond-mat.mes-hall].
- [41] Y. Zhang, Y.-W. Tan, H. L. Stormer, and P. Kim, *Nature* **438**, 201 (2005), arXiv:cond-mat/0509355 [cond-mat.mes-hall].
- [42] K. J. Tielrooij, J. C. W. Song, S. A. Jensen, A. Centeno, A. Pesquera, A. Zurutuza Elorza, M. Bonn, L. S. Levitov, and F. H. L. Koppens, *Nature Physics* **9**, 248 (2013).
- [43] D. Brida et al., *Nature Communications* **4**, 1987 (2013).
- [44] K. S. Kim, Y. Zhao, H. Jang, S. Y. Lee, J. M. Kim, K. S. Kim, J.-H. Ahn, P. Kim, J.-Y. Choi, and B. H. Hong, *Nature* **457**, 706 (2009).
- [45] S. Bae et al., *Nature Nanotechnology* **5**, 574 (2010).
- [46] J. N. Bahcall, *Phys. Rev.* **C56**, 3391 (1997), arXiv:hep-ph/9710491 [hep-ph].
- [47] R. Essig, J. Mardon, and T. Volansky, *Phys. Rev.* **D85**, 076007 (2012), arXiv:1108.5383 [hep-ph].
- [48] M. C. Smith et al., *Mon. Not. Roy. Astron. Soc.* **379**, 755 (2007), arXiv:astro-ph/0611671 [astro-ph].
- [49] S. Reddy, M. Prakash, and J. M. Lattimer, *Phys. Rev.* **D58**, 013009 (1998), arXiv:astro-ph/9710115 [astro-ph].
- [50] S. Kim, I. Jo, D. C. Dillen, D. A. Ferrer, B. Fallahazad, Z. Yao, S. K. Banerjee, and E. Tutuc, *Phys. Rev. Lett.* **108**, 116404 (2012).
- [51] R. Essig, T. Volansky, and T.-T. Yu, *Phys. Rev.* **D96**, 043017 (2017), arXiv:1703.00910 [hep-ph].
- [52] G. J. Feldman and R. D. Cousins, *Phys. Rev.* **D57**, 3873 (1998), arXiv:physics/9711021 [physics.data-an].
- [53] A. Boyarsky, J. Lesgourgues, O. Ruchayskiy, and M. Viel, *JCAP* **0905**, 012 (2009), arXiv:0812.0010 [astro-ph].
- [54] N. Palanque-Delabrouille, C. Yche, N. Schenberg, J. Lesgourgues, M. Walther, S. Chabanier, and E. Armengaud, (2019), arXiv:1911.09073 [astro-ph.CO].
- [55] A. Garzilli, O. Ruchayskiy, A. Magalich, and A. Boyarsky, (2019), arXiv:1912.09397 [astro-ph.CO].
- [56] S. Dodelson and L. M. Widrow, *Phys. Rev. Lett.* **72**, 17 (1994), arXiv:hep-ph/9303287 [hep-ph].
- [57] X.-D. Shi and G. M. Fuller, *Phys. Rev. Lett.* **82**, 2832 (1999), arXiv:astro-ph/9810076 [astro-ph].
- [58] A. E. Nelson and J. Scholtz, *Phys. Rev.* **D84**, 103501 (2011), arXiv:1105.2812 [hep-ph].
- [59] P. Arias, D. Cadamuro, M. Goodsell, J. Jaeckel, J. Redondo, and A. Ringwald, *JCAP* **1206**, 013 (2012), arXiv:1201.5902 [hep-ph].
- [60] P. W. Graham, J. Mardon, and S. Rajendran, *Phys. Rev.* **D93**, 103520 (2016), arXiv:1504.02102 [hep-ph].
- [61] L. Visinelli and P. Gondolo, *Phys. Rev.* **D81**, 063508 (2010), arXiv:0912.0015 [astro-ph.CO].
- [62] H. Baer, K.-Y. Choi, J. E. Kim, and L. Roszkowski, *Phys. Rept.* **555**, 1 (2015), arXiv:1407.0017 [hep-ph].
- [63] D. J. E. Marsh, *Phys. Rept.* **643**, 1 (2016), arXiv:1510.07633 [astro-ph.CO].
- [64] L. Covi and J. E. Kim, *New J. Phys.* **11**, 105003 (2009), arXiv:0902.0769 [astro-ph.CO].
- [65] S. Dimopoulos, G. D. Starkman, and B. W. Lynn, *Phys. Lett.* **168B**, 145 (1986).
- [66] F. T. Avignone, III, R. L. Brodzinski, S. Dimopoulos, G. D. Starkman, A. K. Drukier, D. N. Spergel, G. Gelmini, and B. W. Lynn, *Phys. Rev.* **D35**, 2752 (1987).
- [67] M. Pospelov, A. Ritz, and M. B. Voloshin, *Phys. Rev.* **D78**, 115012 (2008), arXiv:0807.3279 [hep-ph].
- [68] I. M. Bloch, R. Essig, K. Tobioaka, T. Volansky, and T.-T. Yu, *JHEP* **06**, 087 (2017), arXiv:1608.02123 [hep-ph].
- [69] C. E. Aalseth et al. (CoGeNT), *Phys. Rev. Lett.* **101**, 251301 (2008), [Erratum: *Phys. Rev. Lett.* **102**, 109903 (2009)], arXiv:0807.0879 [astro-ph].
- [70] Z. Ahmed et al. (CDMS), *Phys. Rev. Lett.* **103**, 141802 (2009), arXiv:0902.4693 [hep-ex].
- [71] E. Armengaud et al. (EDELWEISS-II), *JCAP* **1311**, 067 (2013), arXiv:1307.1488 [astro-ph.CO].
- [72] Y. S. Yoon et al. (KIMS), *JHEP* **06**, 011 (2016), arXiv:1604.01825 [hep-ex].
- [73] S. K. Liu et al. (CDEX), *Phys. Rev.* **D95**, 052006 (2017), arXiv:1610.07521 [hep-ex].
- [74] G. Angloher et al. (CRESS-IT), *Eur. Phys. J.* **C77**, 299 (2017), arXiv:1612.07662 [hep-ex].
- [75] D. S. Akerib et al. (LUX), *Phys. Rev. Lett.* **118**, 261301 (2017), arXiv:1704.02297 [astro-ph.CO].
- [76] C. Fu et al. (PandaX), *Phys. Rev. Lett.* **119**, 181806 (2017), arXiv:1707.07921 [hep-ex].
- [77] E. Aprile et al. (XENON100), *Phys. Rev.* **D96**, 122002 (2017), arXiv:1709.02222 [astro-ph.CO].
- [78] K. Abe et al. (XMASS), *Phys. Lett.* **B787**, 153 (2018), arXiv:1807.08516 [astro-ph.CO].
- [79] E. Armengaud et al. (EDELWEISS-III), *Phys. Rev.* **D98**, 082004 (2018), arXiv:1808.02340 [hep-ex].
- [80] T. Aralis et al. (SuperCDMS), (2019), arXiv:1911.11905 [hep-ex].